Supplemental Document

Optics Letters

Single-shot observation of breathers from noise-induced modulation instability using heterodyne temporal imaging: supplement

ALEXANDRE LEBEL,[1] ALEXEY TIKAN,[1,2] STEPHANE RANDOUX,[1] PIERRE SURET,[1] AND FRANCOIS COPIE[1,*]

[1] *Univ. Lille, CNRS, UMR 8523 - PhLAM - Physique des Lasers Atomes et Molécules, F-59000 Lille, France*
[2] *Current address: Institute of Physics, Swiss Federal Institute of Technology Lausanne (EPFL), CH-1015 Lausanne, Switzerland*
[*] *Corresponding author: francois.copie@univ-lille.fr*

This supplement published with The Optical Society on 8 January 2021 by The Authors under the terms of the Creative Commons Attribution 4.0 License in the format provided by the authors and unedited. Further distribution of this work must maintain attribution to the author(s) and the published article's title, journal citation, and DOI.

Supplement DOI: https://doi.org/10.6084/m9.figshare.13374809

Parent Article DOI: https://doi.org/10.1364/OL.408730

Single-shot observation of breathers from noise-induced modulation instability using heterodyne temporal imaging: supplemental document

The purpose of this Supplemental Material is to provide some details about the methods used to extract the amplitude and the phase of the optical signal from the raw data recorded in the experiments. In the first demonstration of the SEAHORSE (spatial encoding arrangement with hologram observation for recording in single shot the electric field), the field of view was a few tens of picoseconds and aberrations were neglected [1].
In this Letter, we extend the field of view up to 200 ps and we demonstrate that aberrations induced by the third order dispersion can be significantly compensated in the data analysis.
The theoretical background needed to describe the operation of the SEAHORSE is briefly given in Sec. I. Details about numerical data processing and aberration compensation are provided in Sec. II.

1. SIGNAL RETRIEVAL IN THE SEAHORSE (THEORY)

The notations used throughout this Supplementary document for the field and the Fourier transform are listed below.

$$\text{Direct Fourier Transform } FT\Big(A(t)\Big) = \tilde{A}(\omega) = \int_{-\infty}^{+\infty} A(t)\, e^{-i\omega t}\, dt \tag{S1}$$

$$\text{Inverse Fourier Transform } FT^{-1}\Big(\tilde{A}(\omega)\Big) = A(t) = \frac{1}{2\pi}\int_{-\infty}^{+\infty} \tilde{A}(\omega)\, e^{i\omega t}\, d\omega \tag{S2}$$

$$\text{Convolution : } \quad A \otimes B(\omega) = \int_{-\infty}^{+\infty} A(\omega')\, B(\omega-\omega')d\omega' \tag{S3}$$

$S(t)$ is the slowly-varying amplitude of the electric field $e(t) = S(t)\, e^{i(\omega_0 t)} + c.c.$ under study:

$$\begin{aligned} s(t) &= |S(t)| \\ S(t) &= s(t)\, e^{i\phi(t)} \end{aligned}$$

The slowly-varying amplitude of the pump pulse is $P(t)$. The Fourier components of the chirped pump pulse read :

$$\begin{aligned} p(\omega) &= |\tilde{P}(\omega)| \\ \tilde{P}(\omega) &= p(\omega)\, e^{-i\,\tilde{\phi}_P(\omega)} \\ \tilde{\phi}_P(\omega) &= \frac{B_2}{2!}\omega^2 + \frac{B_3}{3!}\omega^3 \end{aligned}$$

B_2 is the group velocity dispersion (GVD) experienced by the pump pulse in the regenerative amplifier (Astrella, Coherent)
B_3 is the third order dispersion (TOD) experienced by the pump pulse.

In the BBO crystal, the pump intensity is much higher than the signal intensity. In the approximation of weak conversion, the field generated by sum frequency generation (SFG) is proportional to $P(t)$ and $S(t)$ [2]

$$SFG(t) \propto S(t)\, P(t) \tag{S4}$$

In the SEAHORSE, a monochromatic reference beam is also launched into the BBO crystal and the SFG between the pump and the reference provides a field that is simply proportional to $P(t)$:

$SFG_R(t) \propto P(t)$.

The second part of the SEAHORSE is made of a single-shot spectrum analyser. We thus measure the modulus of $\widetilde{SFG}(\omega)$ and the relative phase between $\widetilde{SFG}(\omega)$ and $\widetilde{SFG_R}(\omega)$.

Finally, the recorded data $\tilde{X}(\omega)$ thus reads :

$$\tilde{X}(\omega) = \left[\tilde{S}(\omega) \otimes \tilde{P}(\omega)\right] e^{i\tilde{\phi}_P(\omega)} \tag{S5}$$

$$\begin{aligned}
\tilde{X}(\omega) &= \int_{-\infty}^{+\infty} \tilde{S}(\omega')\, p(\omega-\omega')\, \exp\left[-i\frac{B_2}{2}(\omega-\omega')^2 - i\frac{B_3}{6}(\omega-\omega')^3\right] \exp\left[+i\frac{B_2}{2}\omega^2 + i\frac{B_3}{6}\omega^3\right] d\omega' \\
\tilde{X}(\omega) &= \int_{-\infty}^{+\infty} \tilde{S}(\omega')\, p(\omega-\omega')\, \exp\left[+iB_2\omega\omega' - i\frac{B_2}{2}\omega'^2 + i\frac{B_3}{2}\omega^2\omega' - i\frac{B_3}{2}\omega\omega'^2 + i\frac{B_3}{6}\omega'^3\right] d\omega'
\end{aligned}$$

Parameters of the experiments

B_2	=	$1.437\,\mathrm{ps}^2$
B_3	=	$-2.688\,10^{-3}\,\mathrm{ps}^3$
ω_{max} of the pump	$\approx$	$2\pi \times 7\,\mathrm{THz}$
ω'_{max} of the signal	$\approx$	$2\pi \times 0.2\,\mathrm{THz}$
$B_3(\omega'_{max})^3/6$	$\approx$	9.10^{-4}
$B_3(\omega'_{max})^2\omega_{max}/2$	$\approx$	0.09

We neglect the last two terms in the integral. Moreover, as $\omega_{max} \gg \omega'_{max}$ one can approximate $\tilde{p}(\omega-\omega') \approx \tilde{p}(\omega)$. Finally, one gets :

$$\tilde{X}(\omega) = p(\omega) \int_{-\infty}^{+\infty} \tilde{S}(\omega') \exp\left[-i\frac{B_2}{2}\omega'^2\right] \exp\left[+i\left(B_2\omega + \frac{B_3}{2}\omega^2\right)\omega'\right] d\omega' \tag{S6}$$

Assuming stationarity of the statistics of the random signal $S(t)$, the Fourier components are $\delta-$correlated : $\langle \tilde{S}(\omega')\tilde{S}^*(\omega'')\rangle = N(\omega')\delta(\omega'-\omega'')$. By averaging the data over many realizations, we measure $\tilde{p}(\omega)$:

$$p(\omega) = \sqrt{\frac{\langle|\tilde{X}(\omega)|^2\rangle}{P_0}} \quad \text{where} \quad P_0 = \int N(\omega)\, d\omega \tag{S7}$$

We define

$$\begin{aligned}
\tilde{X}'(\omega) &= \tilde{X}(\omega)/\tilde{p}(\omega) && \text{(S8)} \\
t &= B_2\omega + \frac{B_3}{2}\omega^2 && \text{(S9)} \\
Y(t) &= \tilde{X}\left[\omega(t)\right] && \text{(S10)}
\end{aligned}$$

Eq. (S6) finally reads:

$$Y(t) = \int_{-\infty}^{+\infty} \tilde{S}(\omega') \exp\left[-i\frac{B_2}{2}\omega'^2\right] \exp\left[+i\omega' t\right] d\omega') \tag{S11}$$

Final data analysis

Starting from Eq.(S11), the signal $S(t)$ is retrieved by using the simple algorithm:

1/ Compute $\tilde{Y}(\omega)$, the Fourier transform of $Y(t)$
2/ Apply the operator of propagation $e^{+iB_2\omega^2/2}$
3/ Perform the inverse Fourier transform

It is important to emphasize that in this algorithm, the influence of B_3 on the spectral encoding of time $t(\omega) = B_2\omega + \frac{B_3}{2}\omega^2$ is compensated. On the contrary, we neglect here the influence of B_3 on the phases in the integral. The study of these aberrations in the case of signal with broader spectrum is beyond the scope of this Letter and this point deserves further investigations.

2. NUMERICAL PROCESSING AND ABERRATIONS COMPENSATION :

A. Calibration of time

The SEAHORSE technique is based on the spectral encoding of the signal. The spectral profile of the SFG signal is observed on a sCMOS camera where the frequency components are equally spaced on the x axis by means of a simple grating. A given pixel p_x of the horizontal axis corresponds to a given frequency ω and thus to a given time through Eq. (S9).

The first step of the analysis is to find the quantitative relationship between time and the index px of the pixel:

$$t = a(px - px_0) + \frac{b}{2}(px - px_0)^2 \tag{S12}$$

where $a \propto B_2$ and $b \propto B_3$.

a and b are measured by using a double pulse experiment. Two pulses separated by 81.6 ps are generated by launching a picosecond mode-locked laser (Pritel) beam into a Michelson interferometer. The two pulses are recorded by using the SEAHORSE device. Even though the time interval between the two pulses is fixed at the output of the Michelson interferometer, the pixel interval between the two recorded pulses depends on their positions in the window of measurement because $b \neq 0$.

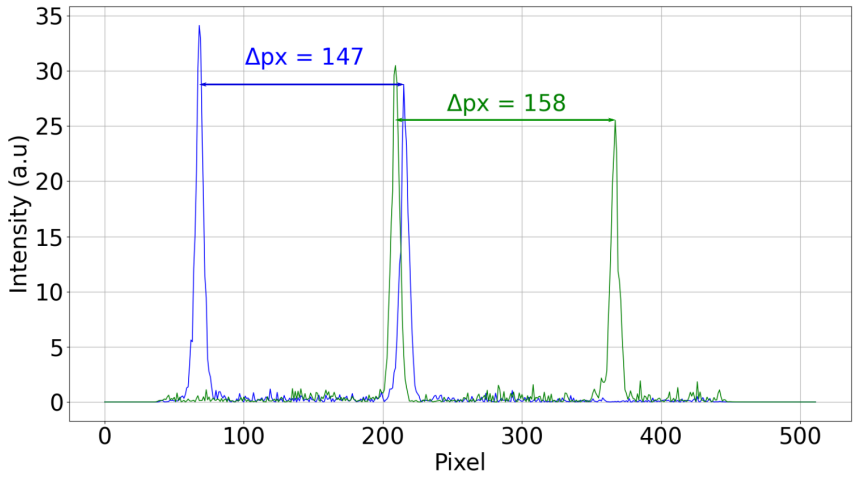

Fig. S1. Double pulse recorded by using the SEAHORSE. The separation Δpx between the two pulses recorded on the camera depends on their mean position $\langle px \rangle$ within the measurement window. Blue and green curve are two different snapshots.

As an example, two different snapshots of the double pulses recorded by using the SEAHORSE are plotted in Fig. S1. By using numerous recorded frames, we measure the distance in pixel between the two pulses as a function of their mean position $\langle px \rangle$ on the camera (see the blue curve in Fig. S2).

By using an optimization procedure, we evaluate px_0, a and b of Eq. (S12) for which the measured interval Δt remains constant over the whole window of observation (see the red curve in Fig. S2):

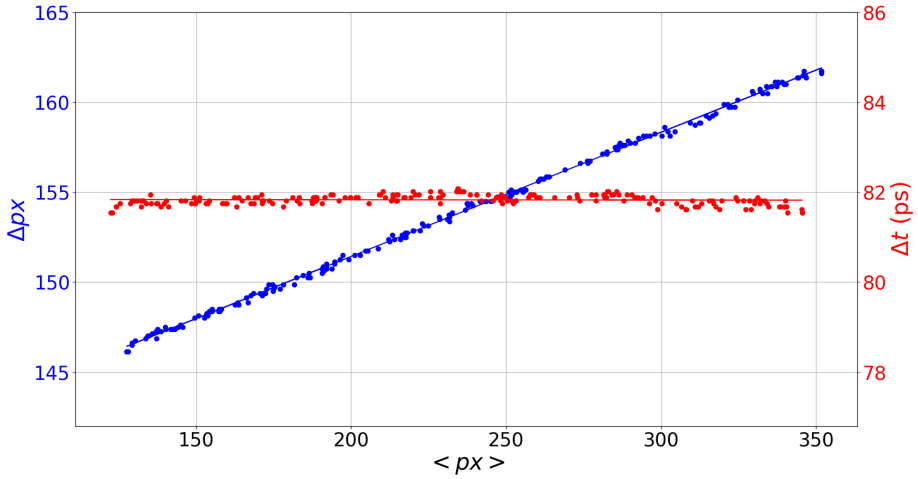

Fig. S2. Blue dot : number of pixels Δpx between the centroids of the two pulses as a function of their mean position $< px >$ in the window. Red dot : time interval between the two pulses Δt computed from the nonlinear pixel to time conversion Eq. (S12). Blue and red solid lines are linear fits related to the same color.

$$a = 5.27 * 10^{-1} \text{ ps / pixel} \quad \text{(S13)}$$

$$b = -1.19 * 10^{-4} \text{ ps / pixel}^2 \quad \text{(S14)}$$

$$px_0 = 232 \quad \text{(S15)}$$

Note that, as expected, the evaluated value of px_0 is close to the centroid of the signal. Note finally that the optimization procedure is an iterative process taking into account the digital focus (see below).

B. Signal retrieval

Above, the correspondence between the time t and the index px of the horizontal pixel of the camera has been established.

In a second step, the intensity and phase of $Y(t)$ [see Eq. (S11)] are retrieved from the raw data recorded onto the camera. A typical single-shot pattern recorded by the camera is plotted in Fig. S3.a). Roughly speaking, for a given time, the intensity $|Y(t)|^2$ corresponds to the sum of the pattern over a vertical line divided by $p(\omega)$ [see Fig. S3.b)]. The phase is encoded in the fringes positions and is retrieved by means of Fourier transform [see Fig. S3.d)]. See [1] for a detailed description of the full procedure.

In a last step, we perform the *Final data analysis* described in Sec. 1. Conceptually, this step corresponds to a *digital focus* analogous in the time domain to the spatial digital holography. The intensity and phase of the retrieved signal is plotted in Fig.S3.(e,f).

It is important to note that the influence of the third order dispersion in the spectral encoding of time is rigorously compensated in the data analysis. On the contrary, for the signals under investigation in this Letter, the influence of the third order dispersion in the digital focus is neglected. The compensation of aberrations for signals with broader spectrum deserves further investigations.

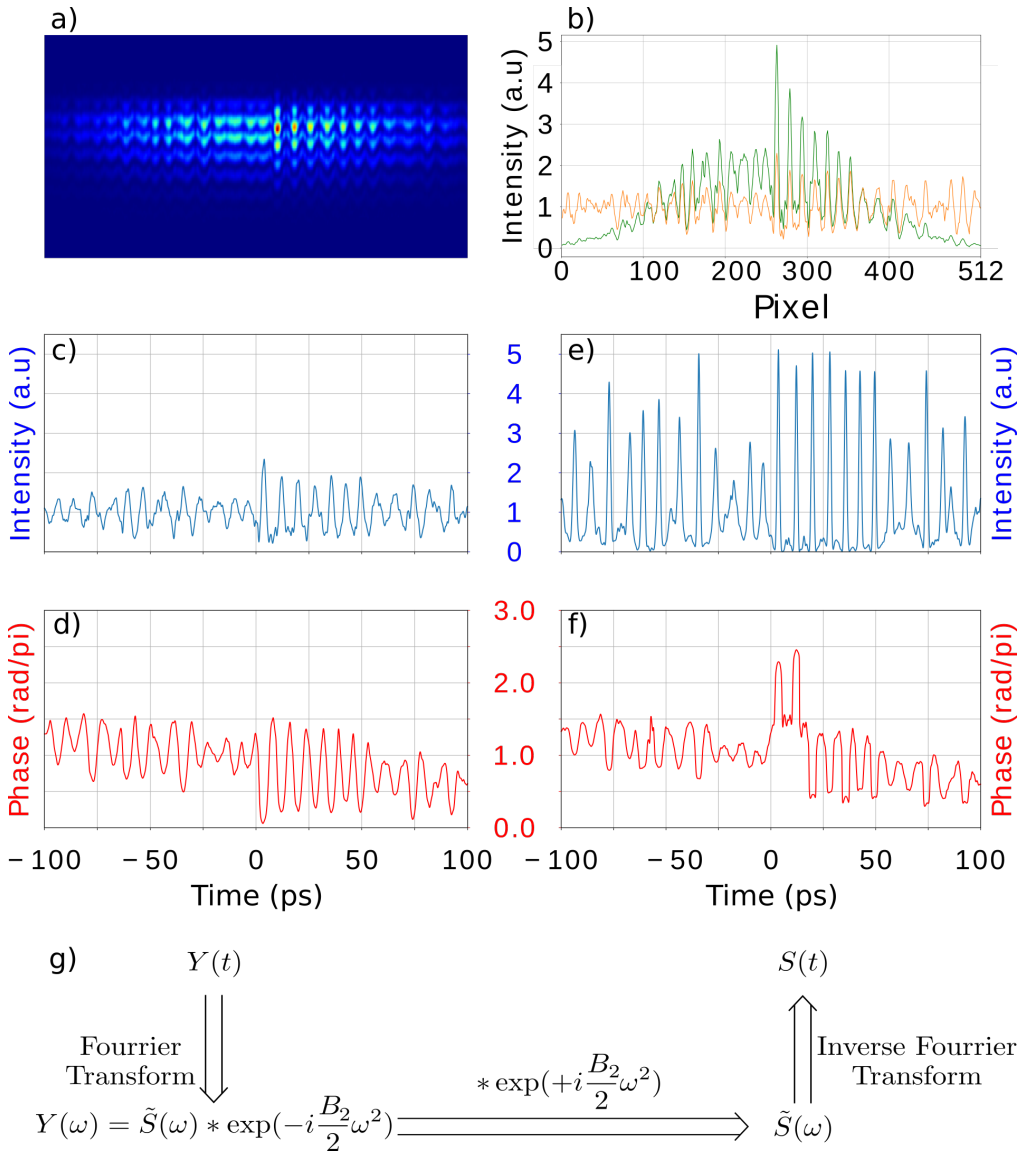

Fig. S3. a) Typical single-shot pattern recorded by the camera. b) Green line : intensity profile extracted from a). Orange : intensity profile divided by the averaged envelop $p(\omega)$. c) Intensity $|Y(t)|^2$ d) Phase of $Y(t)$. In c) and d) the nonlinear pixel to time conversion of Eq. (S12) has been used. e) Intensity of the studied signal $|S(t)|^2$ f) Phase of $S(t)$ g) Principle of the digital focus enabling to retrieve (e,f) from (c,d).

REFERENCES

1. A. Tikan, S. Bielawski, C. Szwaj, S. Randoux, and P. Suret, "Single-shot measurement of phase and amplitude by using a heterodyne time-lens system and ultrafast digital time-holography," Nat. Photonics **12**, 228–234 (2018).
2. R. W. Boyd, *Nonlinear optics* (Academic Press, Amsterdam ; Boston, 2008), 3rd ed.